

Transdimensional surface wave tomography: a one-step approach

Amin Rahimi Dalkhani¹, Xin Zhang², Cornelis^{1,3} Weemstra

¹Delft University of Technology, ²University of Edinburgh, ³Royal Netherlands Meteorological Institute

ABSTRACT

Ambient-noise surface wave tomography has proven to be an effective tool for 3D crustal imaging. Conventionally, a two-step inversion approach is adopted. That is, a first inversion results in separate, frequency-dependent 2D surface-wave velocity maps, upon which local frequency-to-depth inversions are performed. As such, a 3D seismic velocity distribution is recovered effectively. In our case, phase velocities are used. A one-step 3D non-linear algorithm has recently been proposed in a Bayesian framework using reversible jump Markov chain Monte Carlo called transdimensional tomography. This approach has several advantages over the two-step approach, with the most notable being the fact that the one-step approach preserves spatial correlation information in 3D. In this study, we image the shear wave velocity structure of the Reykjanes Peninsula using the recently developed one-step 3D transdimensional surface wave tomography. The transdimensional tomography algorithm uses a variable model parametrization by employing Voronoi cells in conjunction with the reversible jump Markov chain Monte Carlo method. We use the frequency dependent-travel times (with a frequency range of 0.1-0.5 Hz) derived from the recorded ambient noise data to image the area. The results show that the algorithm successfully recovered the velocity structure below the areas sampled with sufficient ray path coverage. The areas with fewer ray paths result in a smoother velocity structure. We observe a few low-velocity anomalies at depths around 4-6 km, likely associated with the high-temperature fields around those depths.

Keywords: Transdimensional tomography, surface wave dispersion, surface wave inversion, Markov chain Monte Carlo, seismic tomography

INTRODUCTION

Seismic surface-wave tomography is a well-known and popular method to obtain the Earth's surface wave velocity structure. Many different techniques and algorithms have been proposed and tested. Conventional linearized or gradient base iterative inversion schemes usually do not include a detailed assessment of the uncertainty (Young et al., 2013). In addition, such schemes require an (a-priori) prescribed cell size, which does not account for spatial variations in sampling (i.e., a non-uniform ray coverage). The transdimensional hierarchical Bayesian method introduced by Bodin et al. (2012) addresses these two limitations. The transdimensional method is a Bayesian inference method relying on reversible jump Markov chain Monte Carlo (rjMCMC) and Voronoi cells to generate samples from the posterior probability distribution of the model given the observed data. Young et al. (2013) and Galetti et al. (2017) used a two-step transdimensional scheme to recover the 3D surface wave velocity structure. The first step involves the recovery of 2D maps of phase velocity using frequency-dependent travel time data employing the 2D transdimensional tomography method of Bodin et al. (2012). This results in laterally varying dispersion curves (phase velocities that are frequency-dependent). These dispersion curves are subsequently inverted separately using a 1D transdimensional approach, which results in a collection of spatially varying 1D velocity models. The estimated depth-dependent velocity models are finally interpolated to build a 3D velocity structure of the subsurface.

Zhang et al. (2018) showed that the two-step inversion scheme could be biased and may cause loss of information. Hence, they proposed a one-step transdimensional approach that uses a 3D discretization of the subsurface using a Voronoi polyhedral tessellation. This method has a comparable computational cost as the two-step transdimensional method but preserves valuable

information and results in a more accurate velocity structure and a better interpretable uncertainty Zhang et al. (2020). Rahimi Dalkhani et al. (2021) reduced the computational costs of the one-step transdimensional method while preserving the non-linearity by updating the ray paths only occasionally (i.e., coincident with the Markov chain thinning level). In this study, we apply the modified one-step transdimensional tomography method (Rahimi Dalkhani et al., 2021) to the ambient noise data recorded over the Reykjanes Peninsula (see Weemstra et al. (2021) for more details).

DATA AND GEOLOGICAL SETTING

There are 83 seismic stations in the region of Reykjanes Peninsula in southwest Iceland that are recording passive seismic noise. The recorded data over a time span of one year has been used for the recovery of surface wave dispersion data (phase velocities) using seismic interferometry by cross correlation (e.g., Weemstra et al., 2021). We aimed at using these picked phase velocity data in 3D transdimensional tomography. Figure 1 shows the station locations available in the region depicted with yellow triangles. As it can be seen, the distribution of stations is non-uniform, i.e., the station coverage is dense in one area while it is sparse in other areas. This implies that the achievable phase-velocity resolution can be expected to vary greatly across the region covered by the seismic array, higher in areas that are more densely covered by stations and decreasing where station density is low.

The tectonic structure on the Reykjanes Peninsula is characterized by six volcanic systems depicted on Figure 1 by red polygons. Four out of six volcanic systems available in the Reykjanes peninsula are within the location of the available seismic stations. Three out of four volcanic systems host a high-temperature zone, in which partial melt are likely to happen. Consequently, low shear wave velocity anomalies are expected to be observed in the tomographic results below these known high-temperature areas.

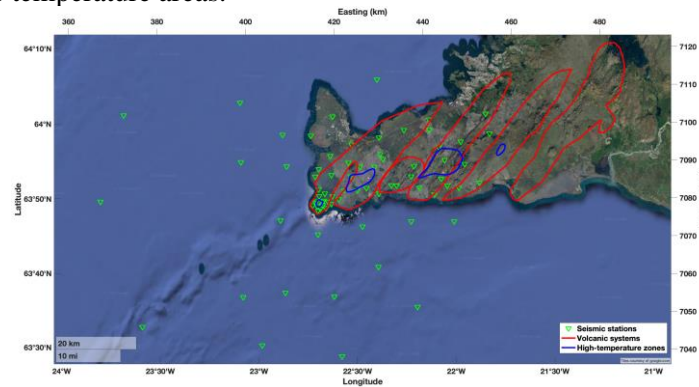


Figure 1. Geographical locations of 83 seismic stations of the RARR. Yellow triangles depict the location of seismic stations. The red polygons are the six volcanic systems. The blue polygons are the known high temperature areas. The left and bottom axes indicate spherical coordinates, whereas the right and the top axes display UTM coordinates.

THE ONE-STEP TRANSDIMENSIONAL SURFACE WAVE TOMOGRAPHY

Transdimensional tomography is a Bayesian inference method that uses Voronoi cells in conjunction with a reversible jump Markov chain Monte Carlo (rjMCMC) algorithm. The reverse jumps allow for a variable number of Voronoi cells, and hence a variable number of parameters. The algorithm involves different types of model perturbations. Specifically, we use four different perturbation types to efficiently sample the posterior distribution (Bodin and Sambridge, 2009): velocity *update*, Voronoi cell *move*, *death*, and *birth*. In addition, we perturb the amplitude of the *noise* to infer the posterior probability of the errors on the measured surface wave travel times (This is introduced by Bodin et al., 2012). These perturbation types allow the model to dynamically adapt to both data density, underlying velocity structure, and travel time noise. At each step of the Markov chain, a new sample is drawn by perturbing the 3D velocity structure (using one of the four perturbation types). The surface wave dispersion data (i.e., the frequency-

dependent travel times) are then calculated to evaluate the following acceptance probability (Bodin and Sambridge, 2009):

$$\alpha(\mathbf{m}'|\mathbf{m}) = \min \left[1, \frac{p(\mathbf{m}')}{p(\mathbf{m})} \times \frac{p(\mathbf{d}_{\text{obs}}|\mathbf{m}')}{p(\mathbf{d}_{\text{obs}}|\mathbf{m})} \times \frac{q(\mathbf{m}|\mathbf{m}')}{q(\mathbf{m}'|\mathbf{m})} \times |\mathbf{J}| \right], \quad (1)$$

where $\alpha(\mathbf{m}'|\mathbf{m})$ is the probability of accepting the proposed model \mathbf{m}' given the current model \mathbf{m} , $\frac{p(\mathbf{m}')}{p(\mathbf{m})}$ the prior probability ratio of two models, \mathbf{d}_{obs} the observed data (here these are the frequency-dependent travel times), $\frac{p(\mathbf{d}_{\text{obs}}|\mathbf{m}')}{p(\mathbf{d}_{\text{obs}}|\mathbf{m})}$ the likelihood ratio of the two models, $\frac{q(\mathbf{m}|\mathbf{m}')}{q(\mathbf{m}'|\mathbf{m})}$ the proposal ratio, and \mathbf{J} is the Jacobian matrix, which accounts for (potential) differences in dimensionality between \mathbf{m} and \mathbf{m}' (resulting from a different number of Voronoi cells).

When sufficient samples are drawn from the posterior, we can compute mean, variance, or other statistical measures of the posterior. The first samples of the chain are discarded. This initial sampling is usually referred to as the burn-in period, which is the period that the algorithm needs to reach sufficient mixing of the posterior samples. Since each sample is drawn based on a small perturbation of its previous model, adjacent samples are correlated or similar to each other. To ensure that the drawn samples are uncorrelated, we retain samples every so many some iterations; for example, every 250th sample is retained. This process is usually referred to as ‘thinning’. The dependence of the posterior on the data is encoded in the likelihood function $p(\mathbf{d}_{\text{obs}}|\mathbf{m})$. To evaluate the likelihood of the proposed model given the observed data, and compare this likelihood with the likelihood of the current model in the chain, we need to compute the frequency-dependent travel times in the proposed model. This is achieved by employing the two-step approach detailed in Zhang et al. (2018). First, at each point on the Earth’s surface, the local frequency-dependent dispersion curve is computed using a modal approximation method (Herrmann 2013). As such, we obtain frequency-dependent maps of surface wave velocity. In the second step, we use these maps to compute frequency-dependent travel times using the fast-marching method (Rawlinson & Sambridge 2004).

The transdimensional tomographic method is very flexible when it comes to combining different data scales or different data types. It is self-regularized and self-smooth and hence doesn't require any regularization or smoothing. In addition, model uncertainty is naturally captured in the posterior. Despite these benefits, the high computational cost is still a drawback of the method. Computing frequency-dependent travel times using the fast-marching method contributes most to the computational cost. Once the ray paths are determined, integration of the slowness along each ray path is straightforward and relatively fast. To make the algorithm computationally less demanding, Bodin et al. (2012) updated the ray paths only occasionally (three times, every one million samples). In this way, they partially linearized the algorithm. Rahimi Dalkhani et al. (2021) proposed to update ray paths at the same level of Markov chain thinning since the ray paths do not change too much in the thinning periods. In this way, we reduce the computational cost significantly while still retaining most of the non-linearity.

RESULTS AND DISCUSSION

Figure 2 shows the posterior mean after one million iterations of 20 sampling Markov chains. The first 400 thousand samples are discarded as the burn-in periods, and the remaining samples are retained at every 250 iterations of each chain to have uncorrelated samples. Ray paths are also updated every 250 iterations. Figure 2(a) is the recovered 3D velocity model. Figure 2(b) is the horizontal slice at the surface of the model. Looking at this figure, one can see that more detailed velocity information is recovered in the areas sampled by a higher density of rays. However, the areas with a smaller number of ray paths are smoothed. Figure 2(c-d) are two vertical profiles of the recovered shear wave velocity structure. Looking at Figure 2(c-d), To the depth of two km, we see a somewhat horizontal layer with a low velocity of around 2km/s. Moreover, from 2km-2.5km, we see a transition between the low and the high velocities. In addition, the velocity for depths more than 2.5 km is generally high (3.6-4 km/s), but low-velocity anomalies beneath the

high-temperature zones are clearly visible, which agrees with our expectation (i.e., high-temperature zones are expected to appear as low shear wave velocity anomalies). However, in the location of the known high-temperature zones at the surface (Figure 2b), contrary to our expectation, the high temperature (HT) zones have relatively high shear wave velocity compared to the surrounding areas. The reason for higher velocities at the surface compared to the surroundings for the HT-areas is the intense alteration in the uppermost 1-2 km and the dense, compact rock, compared to the more permeable and porous rock/lava in the surrounding areas. The pores are filled due to alteration, enhancing the seismic velocities in those areas.

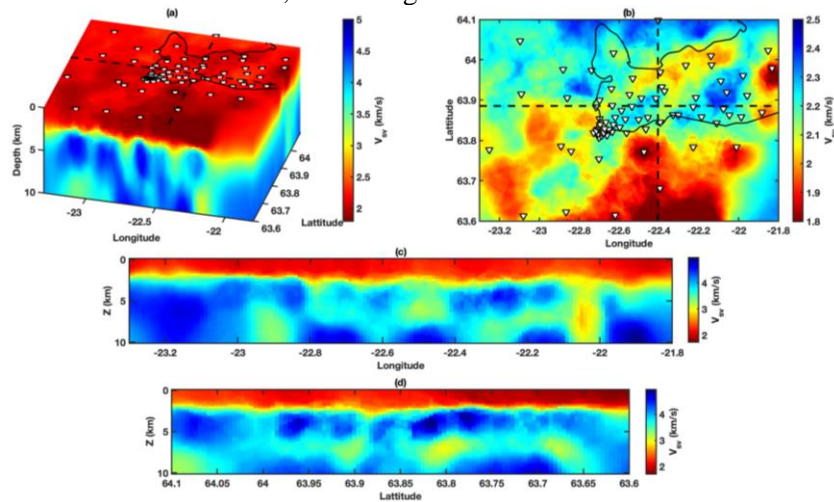


Figure 2. Transdimensional tomographic results of the Reykjanes peninsula. (a) 3D cube of the posterior mean as the recovered velocity model. (b) Horizontal slice at surface. (c) Vertical profiles at the location of the easting dashed line depicted in (b). (d) Vertical profiles at the location of the northing dashed line depicted in (b).

CONCLUSION

We used ambient noise cross-correlations between the Reykjanes seismic array stations to develop a high-resolution shear wave velocity model of the Reykjanes peninsula. We extracted phase velocity dispersion curves and inverted for the shear wave velocity structure. To that end, we used the frequency-dependent phase travel times with a frequency range of 0.1-0.5 Hz. Furthermore, we used a recently developed one-step tomographic algorithm, which is called 3D transdimensional surface wave tomography. Our shear wave velocity model is convincing since it correlates well with previous studies in the area. Low velocity anomalies are clearly observable in the known high temperature zones, which are presumably caused by partial melt. All in all, the shear wave velocity structure of the study area is successfully retrieved by the one-step transdimensional tomography.

REFERENCES

- Bodin, T. and Sambridge, M. (2009) Seismic tomography with the reversible jump algorithm. *Geophysical Journal International*, **178**(3), 1411-1436.
- Bodin, T., Sambridge, M., Tkalcic, H., Arroucau, P., Gallagher, K., & Rawlinson, N. (2012). Transdimensional inversion of receiver functions and surface wave dispersion. *Journal of Geophysical Research*, **117**, B02301.
- Galetti, E., Curtis, A., Baprie, B., Jenkins, D., & Nicolson, H. (2017). Transdimensional Love-wave tomography of the British Isles and shear-velocity structure of the East Irish Sea Basin from ambient-noise interferometry. *Geophysical Journal International*, **208**(1), 36-58.
- Herrmann, R. B. (2013). Computer programs in seismology: An evolving tool for instruction and research. *Seismological Research Letters*, **84**(6), 1081-1088.

- Rahimi Dalkhani, A., Zhang, X., & Weemstra, C. (2021). On the Potential of 3D Transdimensional Surface Wave Tomography for Geothermal Prospecting of the Reykjanes Peninsula. *Remote Sensing*, **13**(23), 4929.
- Rawlinson, N., & Sambridge, M. (2004). Multiple reflection and transmission phases in complex layered media using a multistage fast marching method. *Geophysics*, **69**(5), 1338–1350.
- Weemstra, C., de Laat, J. I., Verdel, A., & Smets, P. (2021). Systematic recovery of instrumental timing and phase errors using interferometric surface waves retrieved from large-N seismic arrays. *Geophysical Journal International* **224**(2), 1028–1055.
- Young, M. K., Rawlinson, N., & Bodin, T. (2013). Transdimensional inversion of ambient seismic noise for 3D shear velocity structure of the Tasmanian crust. *Geophysics*, **78**(3), WB49–WB62.
- Zhang, X., Curtis, A., Galetti, E., & de Ridder, S. (2018). 3-D Monte Carlo surface wave tomography. *Geophysical Journal International*, **215**(3), 1644–1658.
- Zhang, X., Hansteen, F., Curtis, A., & de Ridder, S. (2020). 1-D, 2-D, and 3-D Monte Carlo Ambient Noise Tomography Using a Dense Passive Seismic Array Installed on the North Sea Seabed. *Journal of Geophysical Research: Solid Earth*, **125**(2).